

Supplementary Information

for

Thio-Mayan like Compounds: Excited State Characterization of Indigo Sulfur Derivatives in Solution and Incorporated in Palygorskite and Sepiolite Clays

Raquel Rondão and J. Sérgio Seixas de Melo*

Department of Chemistry, University of Coimbra, P3004-535 Coimbra, Portugal

*corresponding author, email: sseixas@ci.uc.pt

Data Summary

Figure S1. Fluorescence emission and excitation spectra of thioindigo and ciba brilliant pink in toluene, in different concentrations, at 77K.

Figure S2. Evolution of fluorescence excitation spectra of thioindigo in dioxane, with the concentration increasing, and Kubelka-Munk scale diffuse reflectance spectrum of solid thioindigo, T =293K.

Figure S3. Picture of thioindigo (down), and thioindigo mixed with palygorskite (top left) and sepiolite (top right), in a 20% (TI) w/w proportion.

Figure S4. Picture of ciba brilliant pink (down), and ciba brilliant pink mixed with palygorskite (top left) and sepiolite (top right), in a 20% (CBP) w/w proportion.

Figure S5. Diffuse reflectance spectrum (Kubelka-Munk scale) of thioindigo (powder), together with mixtures of palygorskite/thioindigo in different weight percentage proportions, after acid attack, T=293K.

Figure S6. Fluorescence excitation from the mixture thioindigo/palygorskite in different proportions (w/w %), after acid attack, T=293K.

Figure S7. Diffuse reflectance spectrum (Kubelka-Munk scale) of ciba brilliant pink, and mixtures of ciba brilliant pink/palygorskite in different proportions (weight:weight percentage), after acid attack; T=293K.

Figure S8. Fluorescence emission from the ciba brilliant pink/palygorskite mixtures (in w/w proportions), T=293K.

Figure S9. Fluorescence excitation from the mixture ciba brilliant pink/palygorskite in different proportions, T=293K.

Figure S10. Fluorescence decay of thioindigo in palygorskite (20% m/m) at T=293K, with excitation at 450 nm and (A) fitting to a monoexponential decay and (B) fitting to a biexponential decay. Shown as insets are the decay times (τ /ns), pre-exponential factors (a_i), and chi-squared values (χ^2). Also shown are, for a better judgment of the quality of the fits, the weighted residuals and auto-correlation (A.C.) functions.

Tables S1 and S2 with errors associated to the molar extinction coefficient (ϵ_{SS} and ϵ_{TT}) and fluorescence and intersystem crossing quantum yields.

Solvent purification procedure

For thioindigo, at 77K, at higher concentrations, there is an increase in the vibrational resolution, and a narrowing but noisy emission band, likely due to inner-filter effect, Figure S1. For ciba brilliant pink, at the same temperature, the variation in concentration does not induce the same visible changes, likely because the saturation concentration is not achieved in order to form aggregates (Figure S1).

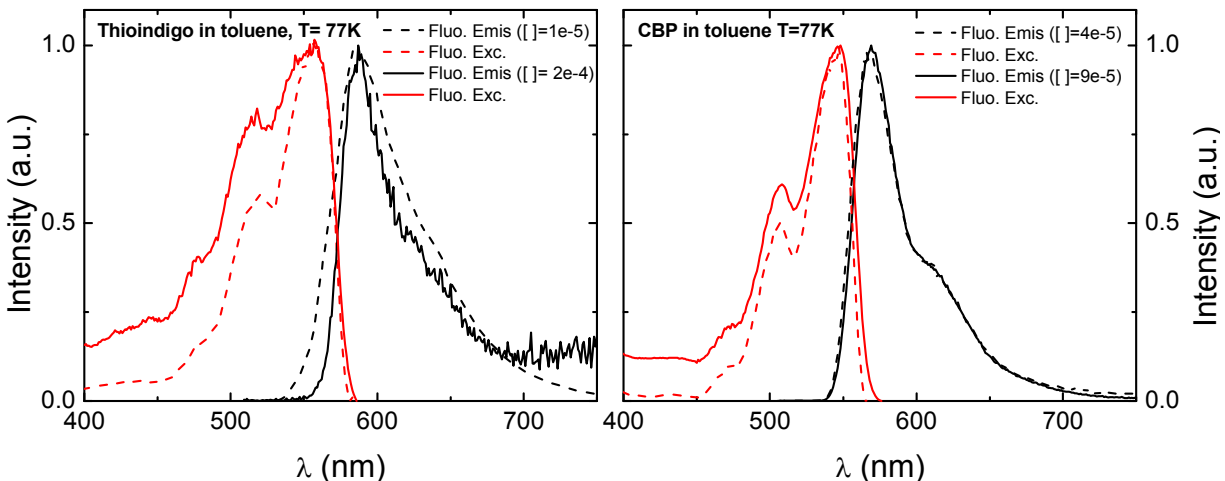


Figure S1. Fluorescence emission and excitation spectra of thioindigo (left hand panel) and ciba brilliant pink (right hand panel) in toluene, in different concentrations, at 77K.

The gradual increase of concentration in thioindigo, does not produce significant changes in the absorption and fluorescence emission bands; however, in the excitation band, collected at the emission maximum, for higher concentrations it is visible the formation of two new bands (with maxima @ 515nm and 550nm), indication the occurrence of aggregation, see Figure S2.

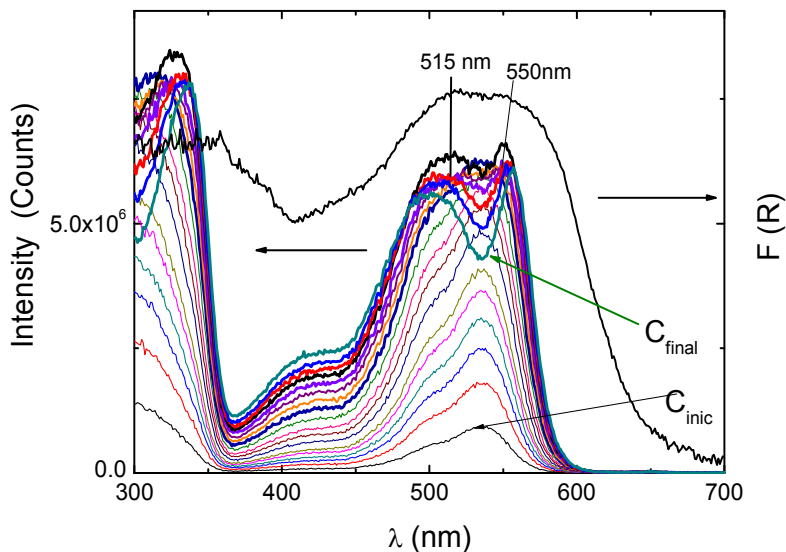


Figure S2. Evolution of fluorescence excitation spectra of thioindigo in dioxane obtained with $\lambda_{em}=590$ nm, with the concentration increasing, and Kubelka-Munk scale diffuse reflectance spectrum of solid thioindigo, T =293K.

The mixture of thioindigo (reddish) with palygorskite and sepiolite produced two different colors – blue and violet, respectively, see Figure S3.

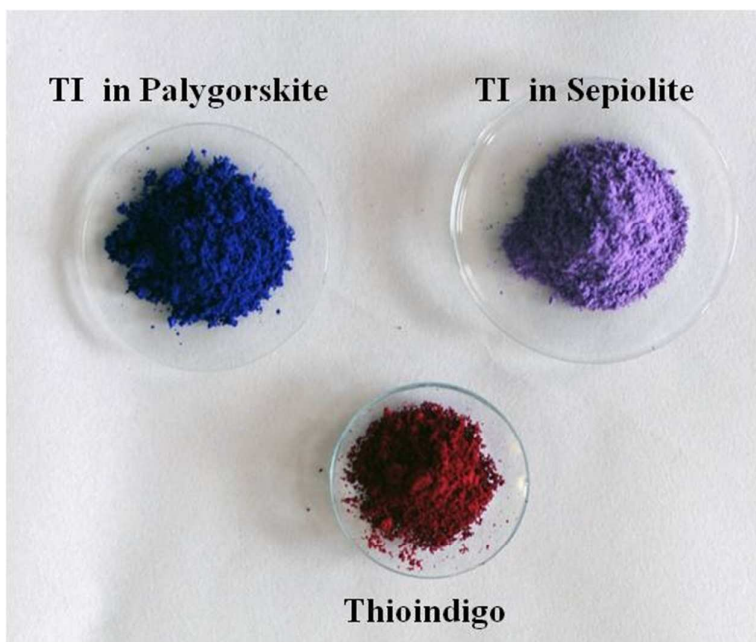


Figure S3. Picture of thioindigo (down), and thioindigo mixed with palygorskite (top left) and sepiolite (top right), in a 20% (TI) w/w proportion.

Ciba brilliant pink, when mixed with the same palygorskite and sepiolite clays, produced two different shades of pink, see Figure S4.



Figure S4. Picture of ciba brilliant pink (down), and ciba brilliant pink mixed with palygorskite (top left) and sepiolite (top right), in a 20% (CBP) w/w proportion.

Comparatively to thioindigo in the powder form, the incorporation in palygorskite clay produces a red shift in the absorption band, which is found identical in all dye/clay proportions (Figures 5 and S5); these absorption spectra are reproduced by the fluorescence excitation spectra (also in Figure 6).

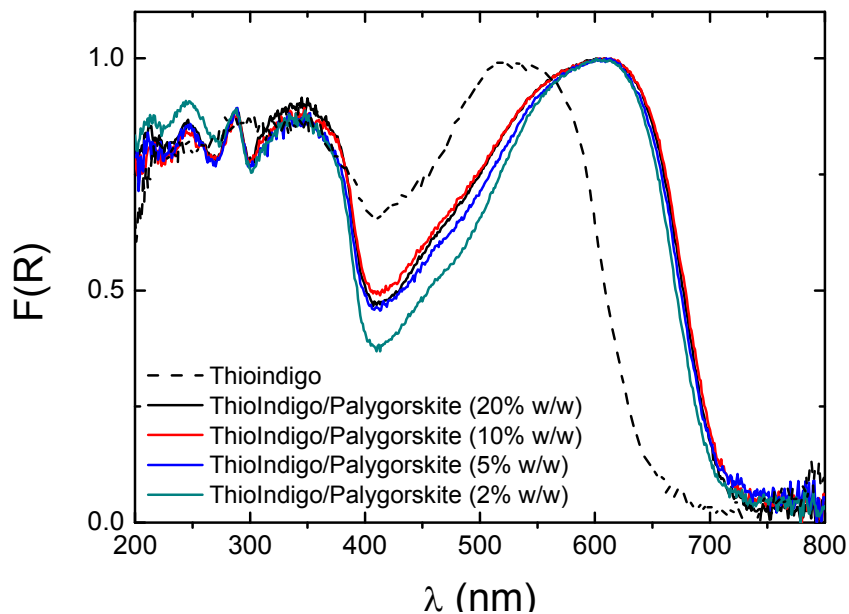


Figure S5. Diffuse reflectance spectrum (Kubelka-Munk scale) of thioindigo (powder), together with mixtures of thioindigo/palygorskite in different weight percentage proportions, after acid attack, T=293K.

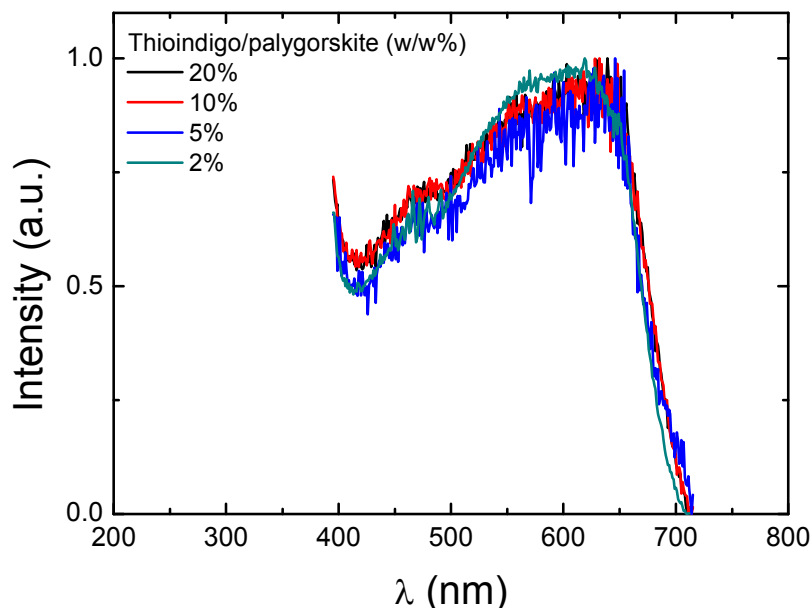


Figure S6. Fluorescence excitation from the mixture thioindigo/palygorskite in different proportions (w/w %), after acid attack, T=293K.

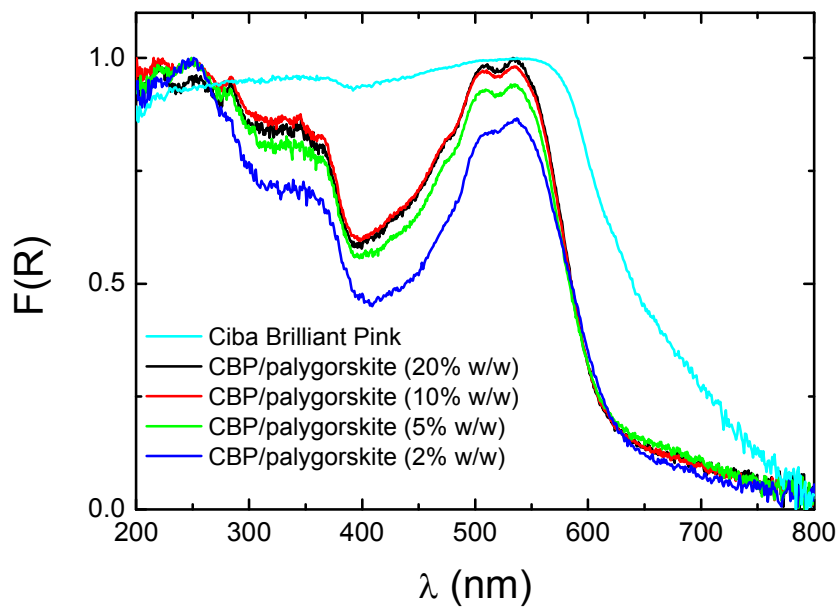


Figure S7. Diffuse reflectance spectrum (Kubelka-Munk scale) of ciba brilliant pink, and mixtures of ciba brilliant pink/palygorskite in different proportions (weight:weight percentage), after acid attack; T=293K.

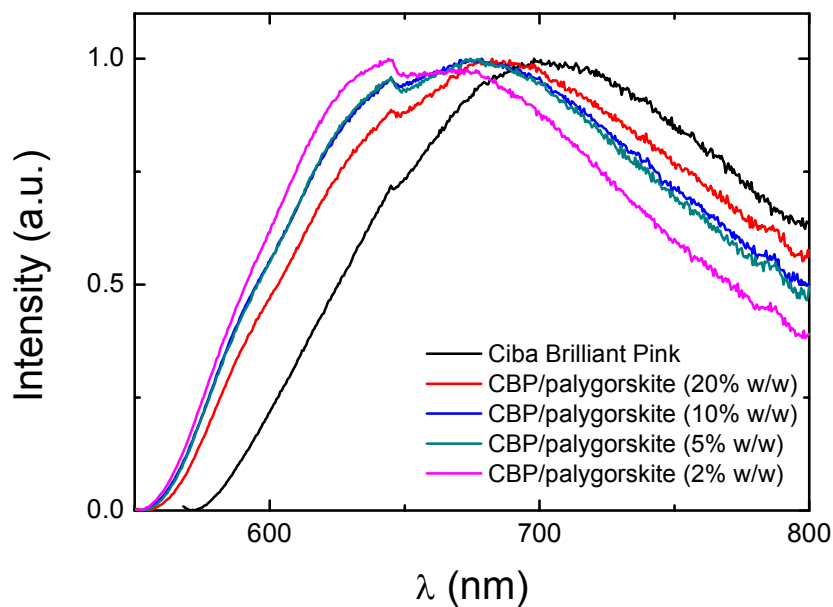


Figure S8. Fluorescence emission from the ciba brilliant pink/palygorskite mixtures (in w/w proportions), T=293K.

The fluorescence excitation spectra of CBP show a more pronounced blue shift relative to the compound in the powder and when mixed in the clay (Figure S9).

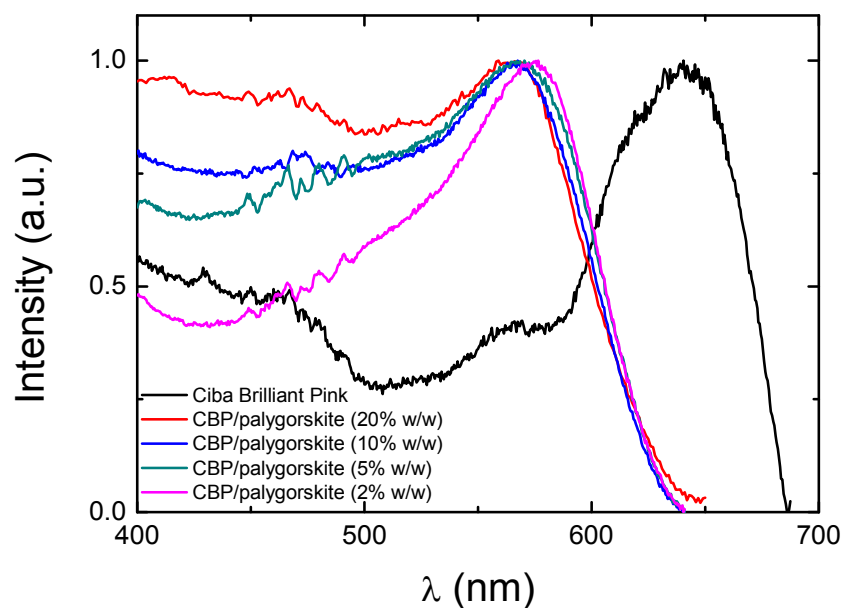


Figure S9. Fluorescence excitation from the mixture ciba brilliant pink/palygorskite in different (w/w) proportions, T=293K.

Figure S10 shows the decays of TI in palygorskite (20% m/m) at T=293K, with excitation at 450 nm and fitting to monoexponential and biexponential decay laws. The bi-exponential fit does not add kind of substantial improvements in the quality of the fit. Moreover the (additional) short component appears associated with a rinsing component which based on our experience of fluorescence in solid state materials it is likely to be a scattering component which we were unable to deconvolute with the instrumental response function signal. Also the difference in the obtained decay time value with a monoexponential fit in Figure 8B (0.170 ps) and in Figure S10 A (0.180 ps) is insignificant and mainly results from the different times scales used: 3.3 ps/ch in the former and 0.816 ps/ch in the latter case.

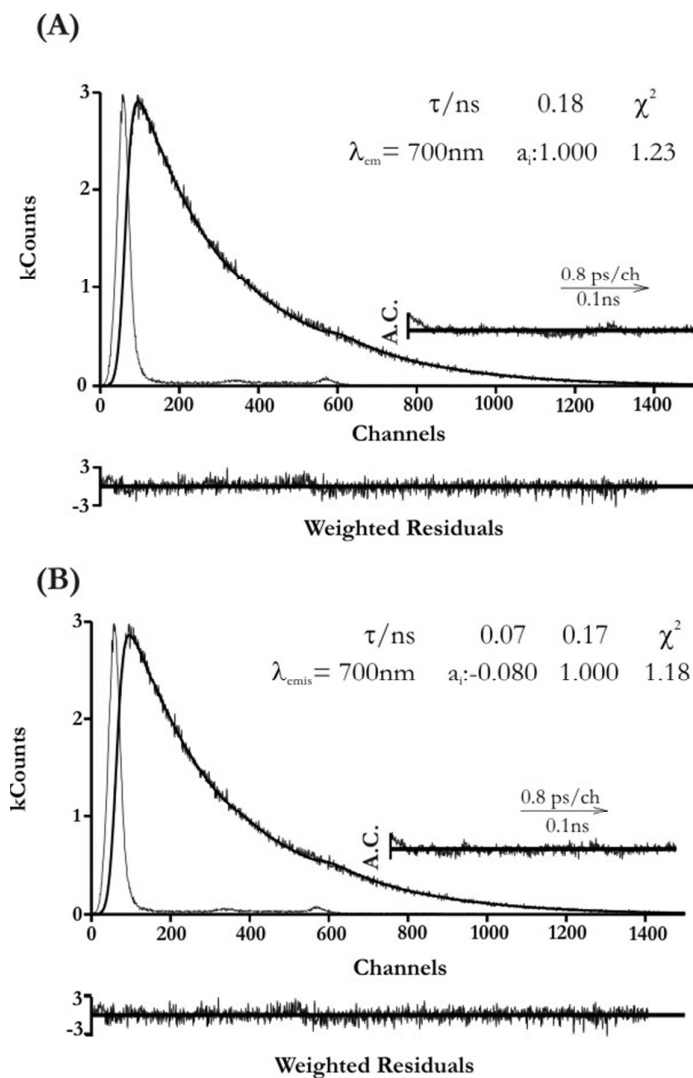


Figure S10. Fluorescence decay of thioindigo in palygorskite (20% m/m) at $T=293\text{K}$, with excitation at 450 nm and (A) fitting to a monoexponential decay and (B) fitting to a biexponential decay. Shown as insets are the decay times (τ/ns), pre-exponential factors (a_i), and chi-squared values (χ^2). Also shown are, for a better judgment of the quality of the fits, the weighted residuals and auto-correlation (A.C.) functions.

Table S1- Spectroscopic Properties for thioindigo and ciba brilliant pink in dioxane, toluene and benzene at 293 K. For indigo the same parameters (obtained in previous works^{1, 4, 47, 48}) are also presented.

Compound /solvent	λ_{\max}^{Abs} (nm) 293 K	λ_{\max}^{Fluo} (nm) 293 K	Δ_{ss} (nm)	ϵ_{ss} (M ⁻¹ cm ⁻¹)	ϵ_{ss} Error %	$\lambda_{\max}^{T_1 \rightarrow T_n}$ (nm)	ϵ_{TT} (M ⁻¹ cm ⁻¹)	ϵ_{TT} Error %
Thioindigo								
Dioxane	536	595	59	12070	3.23	590	12300	0.2
Toluene	542	591	49	14120	0.28	580	15800	1.8
Benzene	543	600	57	13640	0.43	580	14670	2.6
CBP								
Dioxane	530	572	42	7500	2.53	610	11250	7.6
Toluene	537	580	43	7290	4.5	610	11300	9.7
Benzene	537	580	43	5970	6.0	620	13930	11.8
Indigo								
DMF	610	653	43	22140		~640	ND	

Table S2- Photophysical properties including quantum yields (fluorescence, ϕ_F , internal conversion, ϕ_{IC} , triplet formation, ϕ_T , and sensitized singlet oxygen formation, ϕ_{Δ}), lifetimes (fluorescence, τ_F and triplet state, τ_T) and rate constants (radiative, k_F and radiationless, k_{NR}) for thioindigo and ciba brilliant pink in dioxane, toluene and benzene at 293 K. The same parameters (obtained in previous works^{1, 4, 47, 48}) are also given for indigo in DMF.

Compound /solvent	$\phi_F^*(\sigma)$	ϕ_T^*	ϕ_{Δ}^*	ϕ_{IC}^*	τ_T (ns)	τ_F (ns)	k_F^{**} (ns ⁻¹)	k_{NR}^{**} (ns ⁻¹)
Thioindigo								
Dioxane	0.54 (0.01)	0.07 (0.03)	0.06 (0.01)	0.39	328	12.0	0.05	0.04
Toluene	0.69 (0.02)	0.13 (0.001)	0.12 (0.001)	0.18	428	12.3	0.06	0.03
Benzene	0.72 (0.06)	0.12 (0.005)	0.12 (0.02)	0.16	389	12.2	0.06	0.02
CBP								
Dioxane	0.71 (0.03)	0.13 (0.02)	0.06 (0.01)	0.16	372	10.4	0.07	0.03
Toluene	0.70 (0.04)	0.27 (0.01)	0.15 (0.002)	0.03	374	10.4	0.07	0.03
Benzene	0.73 (0.01)	0.24 (0.01)	0.13 (0.02)	0.03	308	10.3	0.07	0.03
Indigo								
DMF	0.0023	0.0066	0.0012	0.996	~ 30 μ s	0.140	0.016	7.13

* Standard deviation (σ) values associated to at least three independent determinations.

$$**\phi_{IC} = 1 - (\phi_F + \phi_T); k_F = \frac{\phi_F}{\tau_F}; k_{NR} = \frac{1 - \phi_F}{\tau_F}$$

Solvent purification procedure

Toluene and benzene were fractionally distilled from sodium.

Dioxane was stood over iron (II) sulfate for 2 days, under nitrogen inert atmosphere; then water (100 mL) and conc. HCl (14 mL) per liter of dioxane were added. After refluxing for 8-12 h, typically 10-20 pellets of KOH were added to the solution under magnetic stirring; at this stage, two layers are formed. After 4-12 hours the upper phase was moved to a clean flask containing sodium, and refluxed for 1 hour, after which it was fractionally distilled.